C. Raga et al., "Black-Box Model, Identification Technique and Frequency Analysis for PEM Fuel Cell With Overshooted Transient Response," in IEEE Transactions on Power Electronics, vol. 29, no. 10, pp. 5334-5346, Oct. 2014

DOI: https://www.doi.org/10.1109/TPEL.2013.2292599

Black-box Model, Identification Technique and Frequency Analysis for PEM Fuel Cell with Overshooted Transient Response

Carmen Raga, *Student Member, IEEE,* Andrés Barrado, *Member, IEEE,* Antonio Lázaro, *Member, IEEE,* Cristina Fernández, *Member, IEEE,* Virgilio Valdivia, *Member, IEEE,* Isabel Quesada, *Member, IEEE,* Lucía Gauchía, *Member, IEEE*

***Abstract*— Fuel cells are one of the most promising energy sources, especially for onboard applications. However, fuel cells present several drawbacks, such us slow dynamic response, load-dependent voltage and uni-directional power flow, that produce an inappropriate vehicle operation. So, secondary energy sources and power converters must be implemented in order to satisfy fast changes in the current load and to store the energy delivered by the load if regenerative braking is intended. Taking into account the number and nature of the power converters, loads, secondary energy sources, and the possibilities for the control strategies, the design of a power distribution architecture based on fuel cells for transport applications is a complex task. In order to address these architectures, modeling and simulation design tools at system level are essential.**

This paper proposes a complete fuel cell black-box model which reproduces the behavior of a commercial fuel cell with overshooted transient response. The identification technique applied to parameterize the model components, based on manufacturer's datasheets and a test based on load steps, is explained thoroughly. Additionally, if only the fuel cell frequency response and manufacturer's datasheet are available, an alternative parameterization methodology based on the fuel cell frequency response is presented.

The fuel cell black-box model is validated experimentally using a commercial PEM (Proton Exchange Membrane) fuel cell. Two different parameterizations are carried out with the aim of verifying the robustness of both the fuel cell model and the proposed identification methodology.

***Index Terms*— black-box model, fuel cell, identification methodology, power distribution architecture, system level model, transport, vehicles**

I. Introduction

FUEL cells are considered as one of the most attractive distributed energy sources, due to their reliability, the low or none polluting emissions and their low maintenance requirements [1]. A fuel cell is an electrochemical device where a continuous catalytic reaction of hydrogen and oxygen takes place in the presence of an electrolyte. Its behavior is characterized by its slow dynamic response, load-dependent voltage and uni-directional power flow. Despite all these drawbacks, and due to their high energy density, fuel cells can be used in a great variety of applications, as uninterruptible power systems, residential applications, power generation systems or grid connection [2]-[3]. However, there are three main areas of application of fuel cells. The first application field is transportation, which includes airplanes, submarines, buses, trains, cars or motorbikes [4]-[7]. The second main application is portable power supply, from few watts to hundreds of watts [8]-[9]. And finally, the last main application refers to stationary distributed power generation [10].

There are several fuel cell technologies, each of which is better suited for a particular application. Proton Exchange Membrane (PEM) fuel cells are mainly used in distributed generation since they can be placed at almost any site, and in vehicle applications due to their easy and safe operation, lack of damaging emissions, compactness, medium-high power range and low temperature operation. Nowadays the design of power distribution architectures for vehicle applications based on fuel cells is an interesting study field. The unregulated output voltage of fuel cells, which depends on the output current and aging, and their poor dynamic response make necessary the use of energy accumulative systems, such as supercapacitors or batteries [11], and power conditioning converters [12]-[13]. Therefore, depending on the technology, number, and location of both the secondary energy sources and converters, there are a great variety of possibilities for the design of the fuel cell vehicle power distribution architecture. Finally, the number of possibilities grows if control strategies and regenerative braking are also taken into account [14]-[17].

Focusing on the power distribution architecture for fuel cell based vehicles, the dynamic modeling and simulation of the whole system play an important role when targeting to achieve the best performance, avoid instabilities and interactions between regulated converters, accumulative energy systems sizing, control strategy optimization, etc. [18]-[19]. Therefore, the development of an accurate and simple fuel cell model is of utmost importance for the design and analysis of the whole system.

The fuel cell models found in literature can be roughly classified into two groups: analytical models and empirical models. The analytical models [20]-[26] are based on chemical and thermodynamic reactions and they require a deep knowledge of the fuel cell internal operation and electrochemistry, which is not always available to design and

Manuscript received October 8, 2013. This work was supported in part by the Spanish Ministry of Education and Science through the research project SAUCE (DPI: 2009-12501).

C. Raga, A. Barrado, A. Lázaro, C. Fernández, V. Valdivia, I. Quesada, are with the Power Electronics Systems Group, Universidad Carlos III de Madrid, Av. Universidad 30, 28911 Leganés (Spain), (corresponding author to provide phone: 34-91-6248753; fax: 34-91-6249430; e-mail: carmen.raga@uc3m.es).

L. Gauchía is with the Electrical and Computer Engineering Department, Michigan Technological University, 1400 Townsend Dr., Houghton, MI, USA, (e-mail: gauchia@mtu.edu).

system engineers. Additionally, these models manage a great amount of parameters, complex sets of equations and they require high computational times. The empirical models, which are derived from experimental results, reproduce the fuel cell behavior by means of look up tables, empirical expressions that can derive in complex sets of equations, or a reduced set of electrical components [9], [27]-[30].

The accuracy of the model depends not only on the kind of model but also on the parameter identification procedure. There are different methods to parameterize the fuel cell model components, that can be applied to diverse kind of models, from the simpler one based on the V-I curve evaluation, to EIS (Electrochemical Impedance Spectroscopy) technique, which is one of the most extended methods and it requires the use of specialized equipment, or the recently proposed computational intelligence-based algorithms such as genetic algorithms, particle swarm optimization algorithms and harmony search algorithms [31], that require mathematical and programming advanced knowledge, and can be a complex task. Therefore, the fuel cell model development is not an easy activity.

In this paper a simple and precise PEM fuel cell black-box model for system-level simulation is proposed, therefore, a trade-off between simplicity and accuracy has to be taken into account, in order to reach reasonable simulation times. The model reproduces both the static and dynamic behavior of the fuel cell. It also comprises a reduced number of passive components and does not require a deep knowledge of the internal fuel cell electrochemical phenomena. The model is parameterized applying an identification methodology based on manufacturer's datasheets and simple measurements in the time domain, therefore only common-use equipment is needed. A prior proposal of this model was presented in [32].

The paper is organized as follows. Section II describes in general terms different fuel cell model topologies, the proposed model and the identification methodology. Section III analyzes the fuel cell response in the frequency domain. Section IV describes the model validation by means of experimental results and finally, the conclusions of this paper are presented in section V.

II. Fuel Cell Model

When a load current step is applied to a fuel cell, the fuel cell voltage transient response can be classified into two types: overshooted and overdamped [33], as depicted in Fig. 1.

The most common one is the overshooted response shown in Fig. 1. In this case, when the current step is applied, the fuel cell voltage firstly exceeds the new steady state value, and after that, this voltage evolves towards the final value with a given time constant value.

The transient response of a PEM fuel cell depends on four major physical factors [33]. Regarding dynamics, these factors are, from slowest to fastest, the stack temperature, the membrane hydration profile, the reactant flow and the general transient phenomena associated with the double capacitive layer effect and the gas diffusion. Most of the dynamic models found in the literature focus on the last two factors.

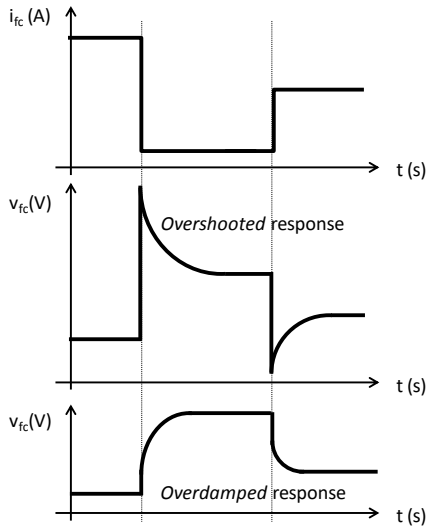

Fig. 1. Overdamped and overshooted response under a load current step for a PEM fuel cell.

The fuel cell models proposed in [33] and [34] are based on functional blocks implemented in Matlab/Simulink [35], in which the model of the double-layer capacity is usually considered as the electrical circuit model of the whole fuel cell. This model can be simplified by neglecting the concentration losses, so the most extended fuel cell model only represents the activation voltage, the double layer effect, and the ohmic losses [36]. Other fuel cell models comprise two RC networks, one for the anode and other for the cathode of the fuel cell, and use Warburg impedances to model diffusion effects, or constant phase elements instead of capacitors [37].

The fuel cell models based on electrical components, that reproduce the fuel cell overshooted transient response, include an inductance in the equivalent circuit, such as the model proposed in [38], which comprises three RC and one RL networks in series, or the simpler model shown in Fig. 2 [39].

One of the three main fuel cell testing techniques is EIS (Electrochemical Impedance Spectroscopy) [40], which is used to parameterize the most of the aforementioned models.

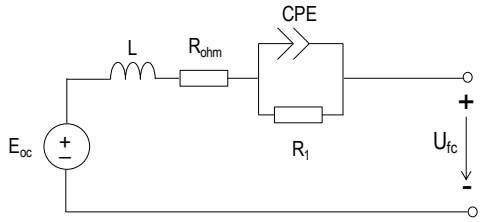

Fig. 2. Simple fuel cell model including an inductor.

The present paper proposes an innovative static and dynamic black-box model of a PEM fuel cell, able to model accurately any type of PEM fuel cell with overshooted transient response, as well as a very simple method for acquiring the fuel cell equivalent circuit parameters. It should be remarked the characteristics provided by this model when compared to those found in literature:

a) The proposed model does not require a deep knowledge of the fuel cell internal operation, electrochemistry, fuel cell internal geometry, physical phenomena and other

performances. Then, from the designer point of view the presented model is more attractive than [20]-[21], [23]-[26], [28], and [33]-[34].

b) The presented model is a black-box model which reproduces the behavior of the fuel cells with overshooted transient response, therefore some proposal like [24], [29] and [36] could be out of the scope of this paper, since they propose fuel cell models under other working conditions, such as overdamped transient responses.

c) Since the model is implemented only with passive components, (three resistors, a capacitor and an inductor), this model avoids the use of sets of equations implemented in additional functional blocks, as well as the combined use of passive components with sets of equations programmed in functional blocks, such as [22] and [30]. Regarding based electrical models, the proposed one, in general, is simpler and smaller. Additionally, the exclusive use of passive components offers a better physical comprehension of the fuel cell operation at system level.

d) The proposed simplified fuel cell model is very easy to parameterize, due to the fact that it is based on a reduced number of simple equations based on time domain measurements and only requires common use equipment.

The simplified PEM fuel cell model is shown in Fig. 3, where E_{oc} is the open circuit voltage, resistors R_s and $R_v(i_{fc})$ model the static I-V curve, and the capacitor C_p, the inductor L and the resistor $R_L(i_{fc})$ model the dynamic behavior of the fuel cell. The diode models the unidirectional power flow of the fuel cell.

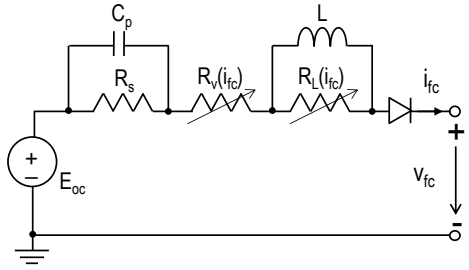

Fig. 3. Simplified overshooted PEM fuel cell model proposed.

The proposed fuel cell model in Fig. 3 intends to be as simple as possible, avoiding the use of variable components. However, in order to be able to develop the proposed simplified fuel cell model, the starting point will be the use of a detailed fuel cell model, in which almost all the components are variable, as shown in Fig. 4.

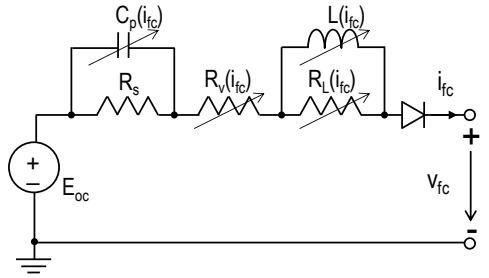

Fig. 4. Initial detailed fuel cell model.

Each passive element of the fuel cell model can be sequentially parameterized, since the main dynamics effects are not coupled, as will be shown next. In order to describe the contribution of each component to the fuel cell behavior, both the static and the dynamic model and the identification methodology (see Fig. 5) will be explained thoroughly in the following sections.

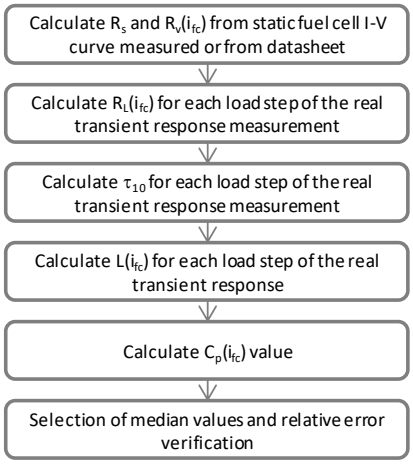

Fig. 5. Proposed identification methodology flowchart.

A. Fuel cell static model and parameters identification

The first value that must be known is the open circuit voltage E_{oc}. This voltage value can be obtained from the manufacturer datasheets or through measurements.

The resistors R_s and $R_v(i_{fc})$ values are calculated from the static I-V curve provided by the manufacturers or by means of measurements on the fuel cell. A typical static characteristic is shown in Fig. 6, where three main areas can be identified: activation region, ohmic region and concentration region.

The value of the resistor R_s is calculated from the fuel cell output voltage considering only the ohmic region (1), where E_{RS} is obtained just extending the ohmic region curve until the v_{fc}(V) axis, see Fig. 6.

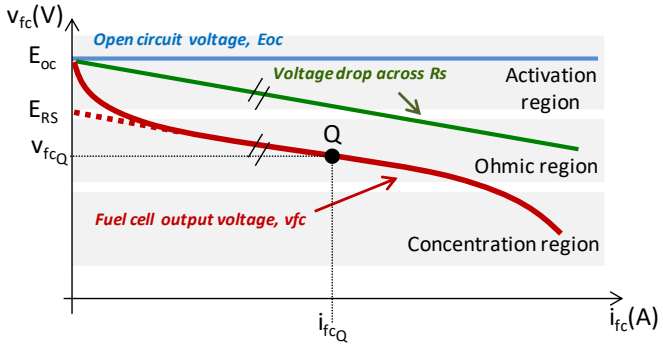

Fig. 6. Main regions in a typical fuel cell current-voltage characteristic.

As the resistor R_s takes a constant value, the resistor $R_v(i_{fc})$ gets variable values depending on the fuel cell current i_{fc}. These values are calculated at each current value from the difference between the open circuit voltage E_{oc}, the voltage drop across the resistor R_s and the fuel cell output voltage $v_{fc}(t)$ (2).

$$R_s = \frac{E_{RS} - V_{fc_Q}}{I_{fc_Q}} \quad (1)$$

$$R_v(i_{fc}) = \frac{E_{oc} - i_{fc} \cdot R_s - v_{fc}}{i_{fc}} \quad (2)$$

At this point, from the manufacturer datasheets or through measurements, the open circuit value E_{oc}, and the resistors R_s and $R_v(i_{fc})$ values have been obtained. The variable resistor $R_v(i_{fc})$ is implemented by means of either a look up table or a mathematical function, matching each fuel cell current value to the corresponding resistor value. The fuel cell static model is shown in Fig. 7.

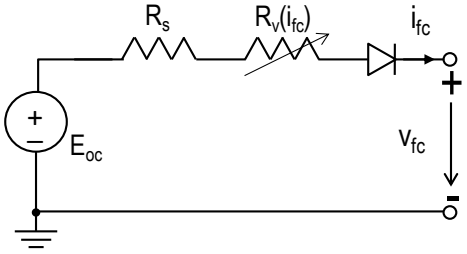

Fig. 7. Static model of the PEM fuel cell.

B. Fuel cell dynamic model and parameters identification for overshooted transient response

Once the static equivalent circuit of the fuel cell is determined, the dynamic model components $R_L(i_{fc})$, $L(i_{fc})$ and $C_p(i_{fc})$ values can be obtained. The development of the fuel cell dynamic model only needs the measurement of the fuel cell output voltage for a set of applied positive and negative load current steps.

The first component that must be calculated is $R_L(i_{fc})$. For that, the voltage transient response of the real fuel cell is compared with the voltage transient response of the fuel cell static model, as depicted in Fig. 8.

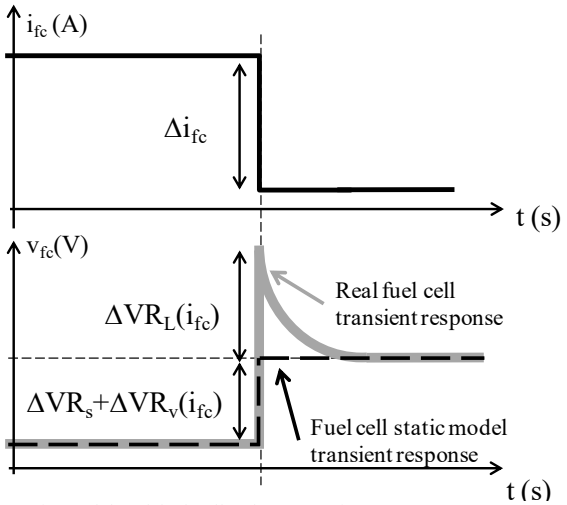

Fig. 8. Static model and fuel cell voltage transient response.

When a load current step takes place, the fuel cell voltage changes instantaneously due to the sum of both, the steady state model resistors R_s and $R_v(i_{fc})$ and the dynamic model resistor $R_L(i_{fc})$. The voltage variation across the resistors R_s and $R_v(i_{fc})$ returns the fuel cell output voltage to its new operation point. Meanwhile, the voltage drop variation across $R_L(i_{fc})$ rises over the new operation point, and then evolves toward it as a first order system, such as shown in Fig. 8.

The resistor $R_L(i_{fc})$ takes a variable value that is calculated by just dividing for each load current step (3) the measured voltage variation $\Delta VR_L(i_{fc})$ by the current-step amplitude Δi_{fc}.

$$R_L(i_{fc}) = \frac{\Delta VR_L(i_{fc})}{\Delta i_{fc}} \quad (3)$$

The next step is to calculate the value of the inductance $L(i_{fc})$. The equation which defines the voltage evolution to a load step is a first order system (4), as shown in Fig. 9.

$$V(t) = V_B + (V_A - V_B) \cdot e^{-t/\tau} \quad (4)$$

The inductance $L(i_{fc})$ value is calculated through the time constant that corresponds to the first 10% of voltage variation after a load current step, τ_{10}. During the parameterization procedure, the fuel cell voltage is measured when a load current step is applied. Therefore, if a negative load current step is applied such as the one presented in Fig. 9, the fuel cell voltage is known and takes the value calculated in (5) just at time t_{10}. This voltage value, $V(t_{10})$, corresponds to the 10% of the voltage drop $\Delta VR_L(i_{fc})$. So, combining expressions (4) and (5), (6) is obtained. Finally, τ_{10} (7) is obtained by solving (6).

$$V(t_{10}) = V_B + 0.9 \cdot (V_A - V_B) \quad (5)$$

$$V_B + 0.9 \cdot (V_A - V_B) = V_B + (V_A - V_B) \cdot e^{-t_{10}/\tau_{10}} \quad (6)$$

$$\tau_{10} = t_{10}/0.105 \quad (7)$$

It should be remarked that, when a positive load current step is applied, the value of $L(i_{fc})$ is calculated analogously since the instant time t_{10} is considered and therefore the time constant τ_{10} equation is also (7), as depicted in Fig. 10.

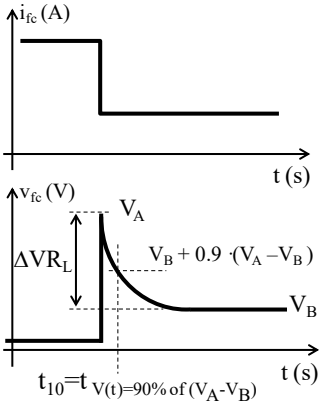

Fig. 9. Negative current load step.

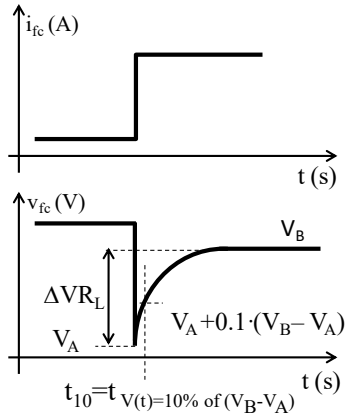

Fig. 10. Positive current load step.

Once the time constant τ_{10} is defined, the next step consists in measuring the time value t_{10} for each load step. Hence, the time constant τ_{10} is derived for each load step by means of (7). Taking into account that this dynamic model is based in an R-L network, using (7) and the set of $R_L(i_{fc})$ values previously calculated, a different value of inductance $L(i_{fc})$ will be obtained for each load current step.

$$L(i_{fc}) = R_L(i_{fc}) \cdot \tau_{10} \quad (8)$$

The result of this identification process is a set of $R_L(i_{fc})$ and $L(i_{fc})$ values. The fuel cell model variable resistors will be more precise if higher number of data is collected.

The last model parameter to identify is the capacitor value $C_p(i_{fc})$, which models the slope of the fuel cell voltage

variation under a load current step, as the Fig. 11 depicts.

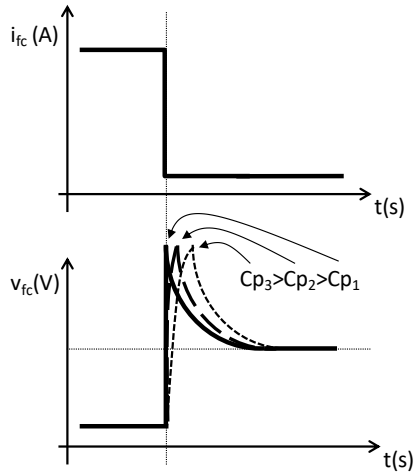

Fig. 11. Capacitor C_p effect on the fuel cell transient response.

If the measured voltage variation is almost instantaneous, then the capacitor $C_p(i_{fc})$ can be neglected. Moreover, in fuel cells with overshooted transient response, the time constant due to the capacitor $C_p(i_{fc})$ is much lower than the time constant due to the inductance $L(i_{fc})$. Otherwise, the capacitor value $C_p(i_{fc})$ is calculated by following a similar method to that used to calculate the inductance $L(i_{fc})$. Therefore, following the previously described methodology, the time constant corresponding to the first 10% of voltage variation after a load current step τ_{10} is defined by the equation (7). Once the time constant is calculated for each load current step, a different value of capacitor $C_p(i_{fc})$ is obtained by means of (9).

$$C_p(i_{fc}) = \tau_{10}/R_s \tag{9}$$

Once the dynamic model components are parameterized, the detailed model of a fuel cell with overshooted transient response is obtained (Fig. 4). However, in order to lighten the fuel cell model implementation in a simulation tool, a simplified fuel cell model using constant values for the capacitor $C_p(i_{fc})$ and the inductance $L(i_{fc})$ is proposed, as Fig. 3 depicts.

In the simplified fuel cell black-box model of Fig. 3, the variable resistances $R_V(i_{fc})$ and $R_L(i_{fc})$ are implemented by means of look up tables or mathematical functions. Regarding to the dynamic components, the inductance L and the capacitor C_p are calculated as the median value of the previously calculated $L(i_{fc})$ and $C_p(i_{fc})$ values respectively, since the median avoids the atypical collected data.

III. Frequency Domain Analysis of the Fuel Cell Model

In the previous section a complete parameterization procedure was presented, however with the aim of deliver additional information, this section analyzes the fuel cell frequency response from the output impedance point of view. The output impedance equation of the complete fuel cell model (10) is derived from the equivalent circuit shown in Fig. 3, assuming that the capacitor $C_p(i_{fc})$ has a not negligible value.

$$Z_{fc}(s) = \frac{(2\cdot\pi\cdot fz_A + s)\cdot(2\cdot\pi\cdot fz_B + s)}{(2\cdot\pi\cdot fp_A + s)\cdot(2\cdot\pi\cdot fp_B + s)} \tag{10}$$

This transfer function (10) presents two poles (fp_A and fp_B) and two zeroes (fz_A and fz_B), resulting in the Bode plot as that depicted in Fig. 12.

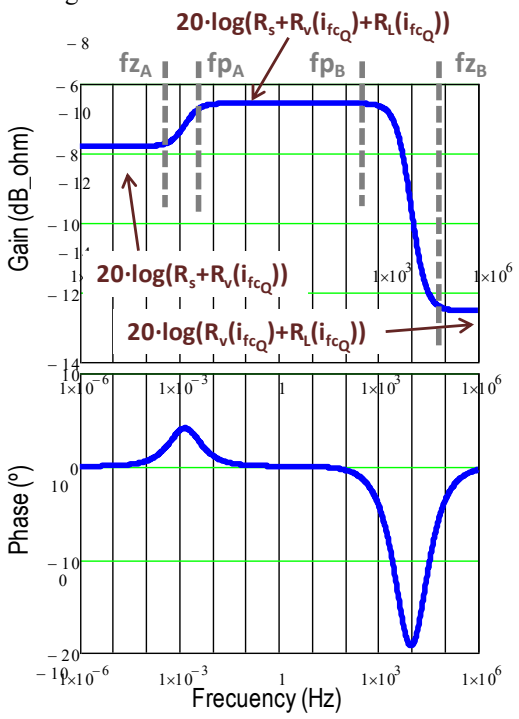

Fig. 12. Fuel cell black-box model output impedance frequency response.

Since the time constant due to C_p is faster than the time constant due to L, then fz_B and fp_B are related to C_p, and fz_A and fp_A are related to L. It can be observed on the frequency response that the frequencies related to each component are far enough, so they can be considered decoupled.

For the analysis at high frequencies, the inductor impedance of the simplified fuel cell black-box model shown in Fig. 3 gets infinite value, so the output impedance transfer function of the previous equivalent circuit is (11).

$$ZB(s) = R_L\left(i_{fc_Q}\right) + R_v\left(i_{fc_Q}\right) + \frac{R_s}{1 + R_s\cdot C_p\cdot s} \tag{11}$$

The simplicity of the previous expression allows calculate the frequencies in which are placed the pole (12) and the zero (13) introduced by the capacitor C_p.

$$fp_B = \frac{1}{R_s\cdot C_p\cdot 2\cdot\pi} \tag{12}$$

$$fz_B = \frac{R_v\left(i_{fc_Q}\right) + R_L\left(i_{fc_Q}\right) + R_s}{\left(R_v\left(i_{fc_Q}\right) + R_L\left(i_{fc_Q}\right)\right)\cdot R_s\cdot C_p\cdot 2\cdot\pi} \tag{13}$$

On the other hand, for the analysis at low frequencies, the capacitor impedance of the simplified fuel cell black-box model shown in Fig. 3 gets zero value, so in this case the output impedance equation is given by (14).

$$ZA(s) = R_s + R_v(i_{fc_Q}) + \frac{R_L(i_{fc_Q})\cdot L\cdot s}{R_L(i_{fc_Q}) + L\cdot s} \tag{14}$$

From (14), the frequencies of the pole (15) and the zero (16) introduced by the inductance L are calculated.

$$fp_A = \frac{R_L\left(i_{fc_Q}\right)}{L \cdot 2 \cdot \pi} \tag{15}$$

$$fz_A = \frac{\left(R_v\left(i_{fc_Q}\right) + R_s\right) \cdot R_L\left(i_{fc_Q}\right)}{\left(R_v\left(i_{fc_Q}\right) + R_L\left(i_{fc_Q}\right) + R_s\right) \cdot L \cdot 2 \cdot \pi} \tag{16}$$

At low frequencies an inductor behaves as a short circuit, and a capacitor acts as an open circuit. On the other hand, at high frequencies an inductor behaves as an open circuit and a capacitor acts as a short circuit. Taking this into account, it can be known the value of the output impedance gain in low (17), medium (18) and high (19) frequencies of the fuel cell black-box model frequency response, as depicted in Fig. 12.

$$|Z_L| = 20 \cdot \log\left(R_s + R_v\left(i_{fc_Q}\right)\right) \tag{17}$$

$$|Z_M| = 20 \cdot \log\left(R_s + R_v\left(i_{fc_Q}\right) + R_L\left(i_{fc_Q}\right)\right) \tag{18}$$

$$|Z_H| = 20 \cdot \log\left(R_v\left(i_{fc_Q}\right) + R_L\left(i_{fc_Q}\right)\right) \tag{19}$$

In case that the capacitor C_p was negligible, (see section II), the complete fuel cell black-box model corresponds to the low frequency model described in this paragraph.

Finally, if only the fuel cell frequency response and the manufacturer datasheet are available in order to parameterize the fuel cell, the alternative procedure to parameterize the fuel cell is the following:

1. Parameterize the resistors R_s and $R_v(i_{fcQ})$ by applying the identification methodology described in section II-A.
2. Calculate the $R_L(i_{fcQ})$ value through the measurement of the gain at high frequency and equation (19).
3. Calculate the L value by measuring the frequency in which the pole fp_A or the zero fz_A is located and use (15) or (16).
4. Repeat steps 1-3 for each one of the operating points considered.

IV. Experimental Model Validation

A model for a commercial Nexa Ballard 1.2kW PEM fuel cell has been derived by means of the proposed procedure.

The test experimental setup is shown in Fig. 13.

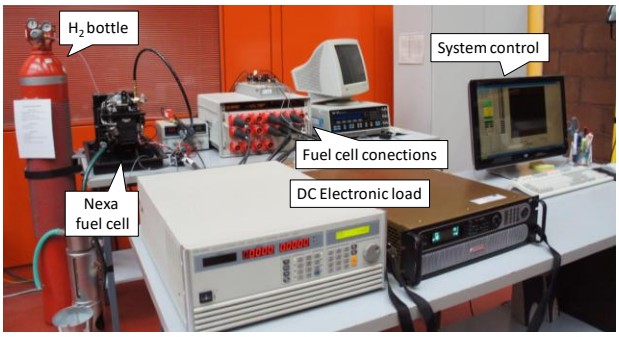

Fig. 13 Experimental setup photograph.

First of all, the fuel cell static model is parameterized from the measured I-V curve as described in section II-A. The calculated value of resistor R_s is 120mΩ, and the obtained values for resistor $R_v(i_{fc})$ are shown in Table I.

Table I

Static Fuel Cell Model Parameters

i_{fc}(A)	$R_v(i_{fc})$ (Ω)	i_{fc}(A)	$R_v(i_{fc})$ (Ω)
1	1.780	25	0.312
2	1.080	30	0.279
3	1.013	35	0.251
4	0.905	40	0.229
5	0.820	42	0.225
8	0.630	43	0.222
10	0.550	44	0.221
15	0.427	45	0.227
20	0.358		

The non-linear nature of the resistor $R_v(i_{fc})$ is shown in Fig. 14.

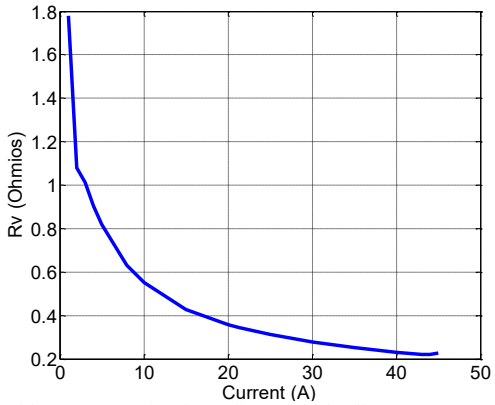

Fig. 14 Variable resistor $R_V(i_{fc})$ depending on fuel cell current.

In Fig. 15 the static behavior of the fuel cell model is compared with the experimental response of the fuel cell, and it can be seen that both I-V curves fit almost exactly.

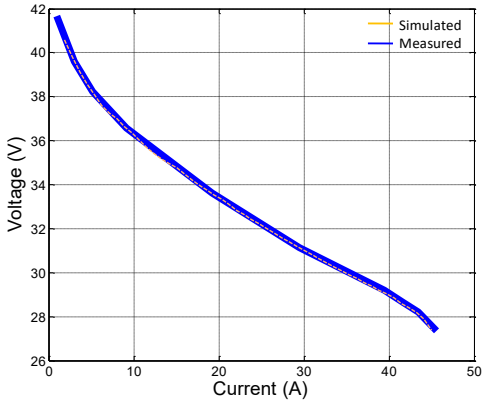

Fig. 15 Comparison between fuel cell I-V curve measured and fuel cell model I-V curve simulated.

In order to parameterize the fuel cell dynamic model components, four different load current profiles have been applied to the PEM fuel cell. The load current profiles are formed by different number and magnitude of current increments, which go from 11% to 88% load range. With the aim of analyzing the influence of both the number and load current steps magnitude over the fuel cell model behavior, two different parameterizations have been carried out.

The sub-section A describes the fuel cell parameterization procedure using the load current profile with the smallest current increments. Afterwards, the fuel cell model behavior is verified comparing the measured data and the model

simulation results with the other three load current profiles.

The sub-section B describes the fuel cell parameterization procedure using the current profile with medium current increments. After that, again, the model behavior is verified through the comparison of the fuel cell model response and the other three measured responses.

A. Parameterization procedure by applying load current increments of 11% load range.

The data measured are shown in Fig. 16, where it can be seen that the load current steps applied to the fuel cell have an 11% of load range.

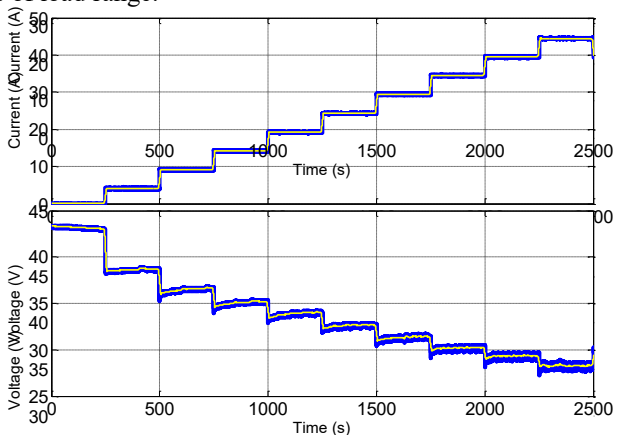

Fig. 16 Nexa fuel cell experimental results, filtered and original measured, used in the identification methodology.

The upper plot in Fig. 16 is the fuel cell current, and the lower one is the fuel cell output voltage. In order to make easier the identification process, the noise in the experimental waveforms has been smoothed by using a symmetric moving average filter. Both the filtered and the original measured data are compared in Fig. 16.

By applying the identification methodology presented in section II-B, the data shown in Table II have been calculated. These data model the variable resistor $R_L(i_{fc})$ and the inductance $L(i_{fc})$. The selected inductance value for the simplified fuel cell model is the median one, L=4.52H. This fuel cell model is oriented to system level simulation, so the capacitor $C_p(i_{fc})$, related to the double layer capacitor phenomena, has been neglected.

TABLE II

DYNAMIC FUEL CELL MODEL PARAMETERS

i_{fc}(A)	τ_{10} (s)	$R_L(i_{fc})$ (mΩ)	$L(i_{fc})$ (H)
4.127	5.012	0.083	3.970
9.156	6.122	0.126	7.352
14.190	4.210	0.113	4.528
19.200	8.320	0.126	10.023
24.230	8.860	0.067	5.688
29.410	7.540	0.092	6.599
34.470	6.200	0.073	4.298
39.450	3.040	0.067	1.947
44.480	1.500	0.026	0.375

The proposed simplified fuel cell black-box model, parameterized as described in section II, is shown in Fig. 17. The model has been implemented in the simulation tool PSIM [41]. The variable resistors $R_v(i_{fc})$ and $R_L(i_{fc})$ can be implemented by using look up tables or mathematical expressions derived from the collected data.

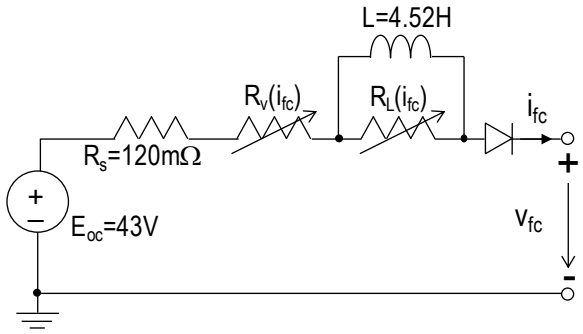

Fig. 17 Nexa fuel cell black-box simplified model.

In order to verify the parameterization procedure, the same set of load current steps used in the parameter identification process has been applied to the fuel cell model. The simulation results are presented together with the measured data in Fig. 18. As can be seen in Fig. 18, a very long sequence of load current steps of 11% load range have been applied at the fuel cell terminals. In all cases, the model fits accurately the measured fuel cell voltage. The third screen in Fig. 18 corresponds to the relative error between the experimental and the simulation results. It can be remarked the good accuracy obtained between the model simulation results and the experimental data, since the relative error is kept within ±2% along the whole test. The error peaks greater than ± 2% that appear in every load current change are due to the different precision that have the simulation tool PSIM and the experimental acquisition data tool dSPACE [42].

As can be seen, even assuming constant L, the experimental and the simulation results fit very accurately.

At this point, it has been demonstrated that the fuel cell model is able to reproduce the experimental results used for its parameterization. Along the next paragraphs the obtained simulation results for other different sets of load current steps are compared with the measured experimental results.

In Fig. 19 a set of load current steps with increments of 11% and 44% load range has been applied. It can be observed that the simulated voltage evolves as the measured one and for most of the steps the relative error is kept within ±2%, except for the first step in which the error is a little higher.

In Fig. 20 a sequence of load current steps of 25% and 50% load range is applied. It is noticeable the good accuracy obtained between the model simulation results and the experimental data, since the relative error is kept within ±4% during the entire test.

Finally, in Fig. 21 two steps of 77% and 88% load change are applied, and even in these conditions the model response is very similar to that of the real fuel cell with a relative error below 5%.

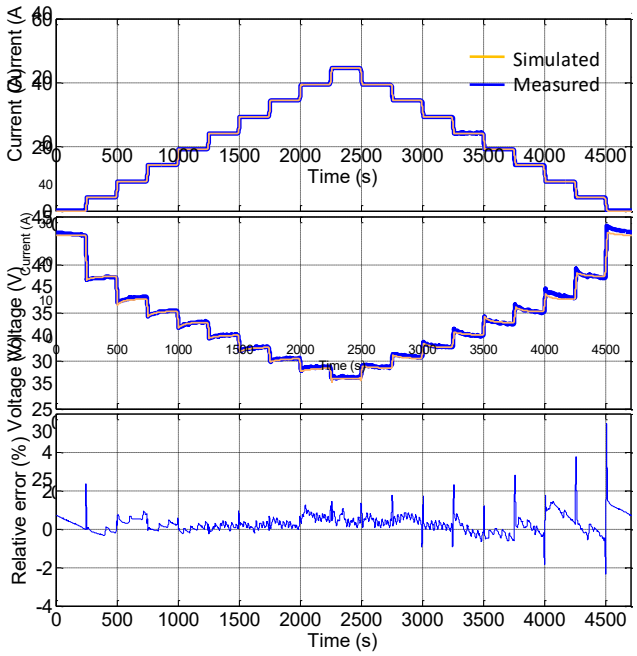

Fig. 18. Nexa fuel cell experimental and model simulation results used in the identification methodology, applying current increments of 11% range.

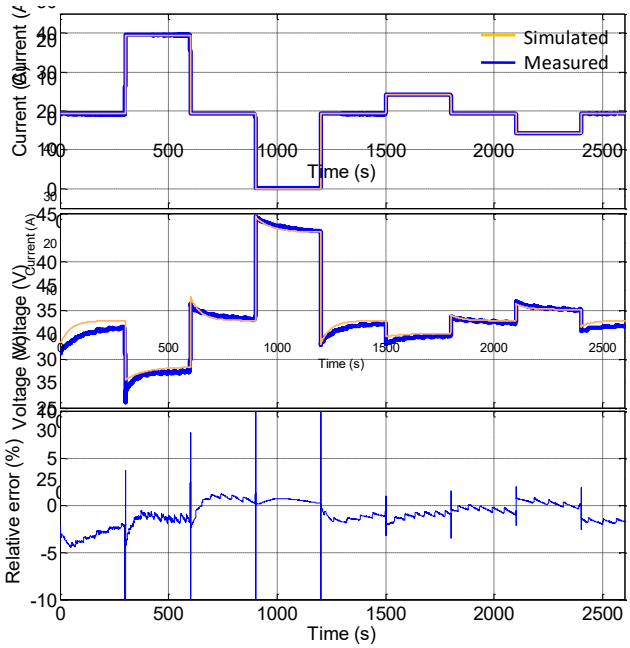

Fig. 19. Nexa fuel cell experimental and model simulation results, applying current increments of 11% and 44% load range.

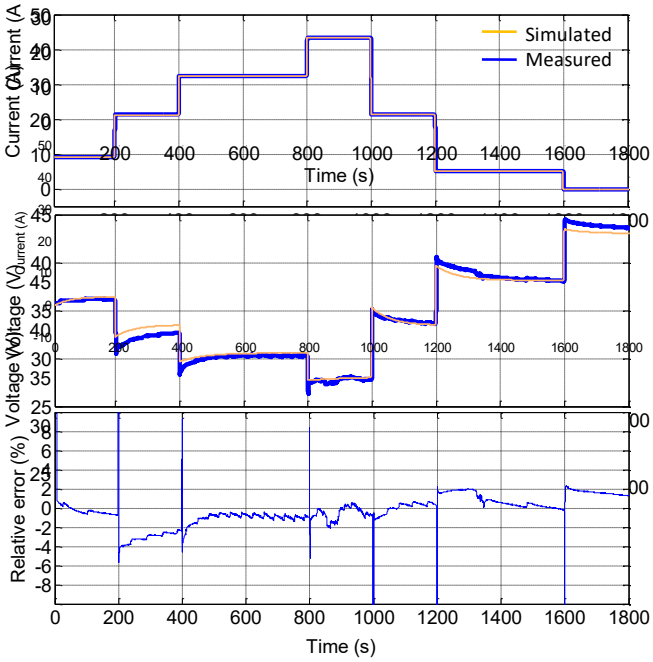

Fig. 20 Nexa fuel cell experimental and model simulation results, applying current increments of 25% and 50% load range.

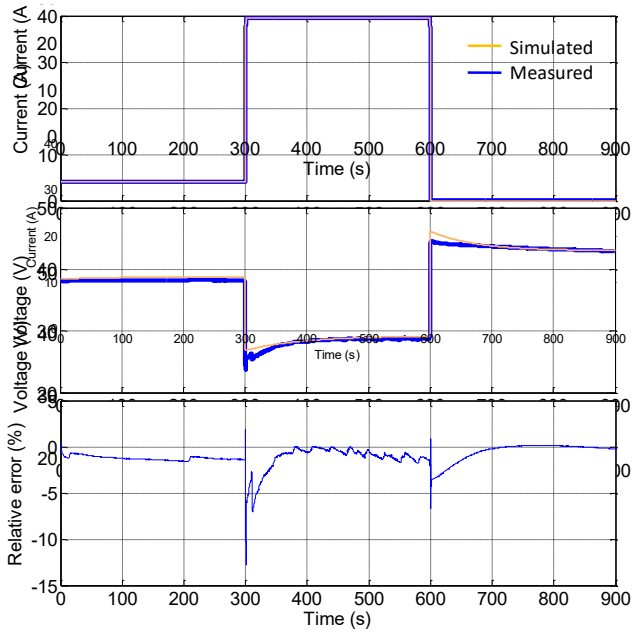

Fig. 21 Nexa fuel experimental and model simulation results, applying current increments of 77% and 88% load range.

It must be reminded that in order to simplify the proposed detailed fuel cell model, the median estimator has been used instead of current dependant parameters for the model components $C_p(i_{fc})$ and $L(i_{fc})$. This means that the values farthest from the median ones will introduce a bigger error than the closest ones in the simulation results. Taking this into account, the difference between the model predicted value and the experimental one observed in the previous figures, especially in figures 20 and 21, could be related to the parameterization procedure but is mainly due to the modeling assumption. Nevertheless, the relative error shows a good accuracy of the modeling.

It can be summarized that the simplified fuel cell black-box model response, parameterized applying current increments of 11% load change, fits with a good accuracy the fuel cell experimental response.

B. Parameterization procedure by applying load current increments of 25% and 50% load change.

In order to determine which set of load current steps suits better the fuel cell identification methodology, the

parameterization process has been carried out for another set of current steps. Additionally in this case the double layer capacitor phenomena is considered. Most of the load current steps of this sequence have 25% load range and have been represented in Fig. 23. The numerical results for the parameterization are given in Table III and the obtained inductance value is L=5.54H.

TABLE III

DYNAMIC FUEL CELL MODEL PARAMETERS: R_L AND L.

i_{fc}(A)	τ_{10} (s)	$R_L(i_{fc})$ (mΩ)	$L(i_{fc})$ (H)
0.900	52.190	0.177	9.235
5.120	54.952	0.132	7.271
9.090	59.524	0.045	2.702
21.230	50.571	0.152	7.710
21.300	25.524	0.056	1.424
32.350	37.619	0.147	5.548
43.410	61.905	0.045	2.767

Analogously, the capacitor value C_p=330mF, has been selected as the median value of the data set shown in Table IV.

TABLE IV

DYNAMIC FUEL CELL MODEL PARAMETER C_P

i_{fc}(A)	τ_{10} (ms)	$C_p(i_{fc})$ (mF)
5.12	41.52	346
9.09	50	421
21.23	37.33	311
32.35	39	330
43.41	34	280

The proposed simplified fuel cell black-box model, parameterized as described in section II, and implemented in the simulation tool PSIM, is shown in Fig. 22. The variable resistors $R_v(i_{fc})$ and $R_L(i_{fc})$ can be implemented by using look up tables or mathematical expressions derived from the collected data.

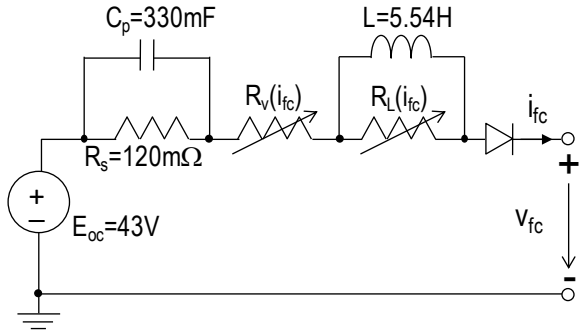

Fig. 22 Nexa fuel cell black-box simplified model including the capacitor C_p.

In Fig. 23 it can be noted that the parameterization procedure has been carried out properly, since the simulation and experimental results fit accurately, with a relative error confined between ±2%.

Finally, the response of the implemented fuel cell model is compared to the experimental data for different sets of load current steps. The simulation results and the experimental data for the current steps (upper screen), fuel cell output voltage (middle screen) and relative error (lower screen) are shown in Fig. 24, Fig. 25 and Fig. 26. In all the considered cases the relative error is kept below 5%, furthermore it can be noted that in the great majority of the current steps the relative error is confined to ±2%. The effect of including in the fuel cell model the double layer capacitance phenomena can be observed in the relative error shown in Fig. 23, Fig. 24, Fig. 25 and Fig. 26. In this case, the obtained relative error in each load current transition is smaller than the obtained in the previous parameterization, in which the capacitor C_p value had been neglected. Therefore the fuel cell model behavior has been improved, reducing the relative error during the load current transitions, and from the system level point of view the response of the fuel cell model has not been modified.

From the obtained results, it can be concluded that there is no significant difference between the responses of the fuel cell model parameterized from the two different sets of current steps. Therefore, the fuel cell black-box model is robust to the number of points needed to define both the inductance $L(i_{fc})$ and the variable resistor $R_v(i_{fc})$ values, and also to the increment values of the load current steps applied in the parameterization procedure.

Regarding the double capacitive layer effect, which constitutes the physical factor with the fastest dynamic, Fig. 27 shows a detail in which the good accuracy between measured and simulated data can be noted.

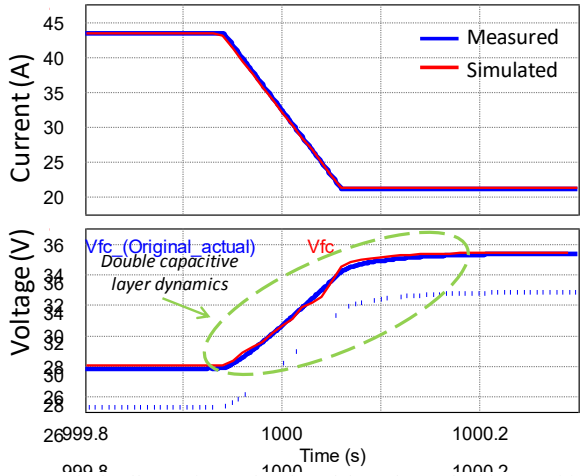

Fig. 27 Nexa fuel cell experimental and model results. A double capacitive layer dynamics detail.

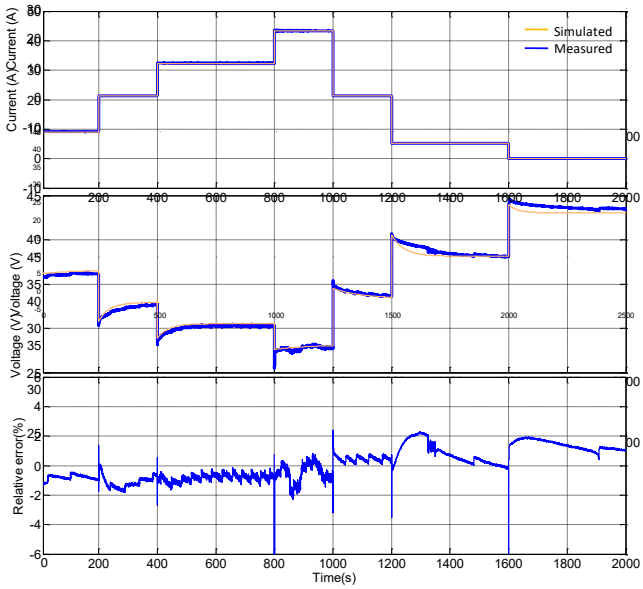

Fig. 23 Nexa fuel cell experimental results used in the identification methodology, and model simulation results.

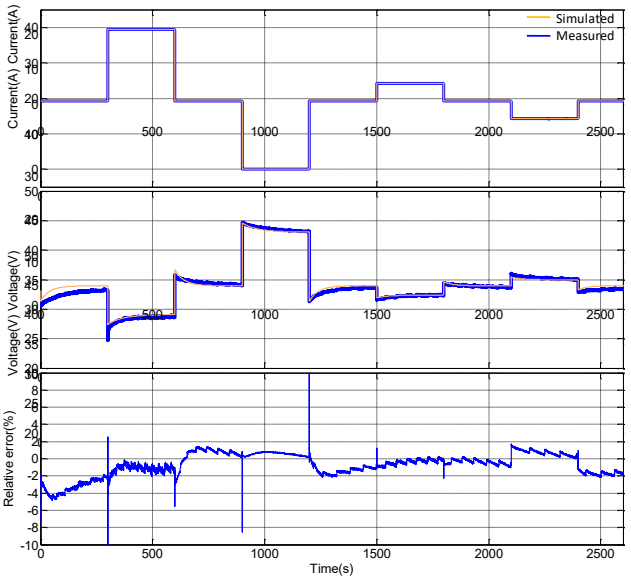

Fig. 24 Nexa fuel cell experimental and model simulation results, applying current increments of 11% and 44% load range.

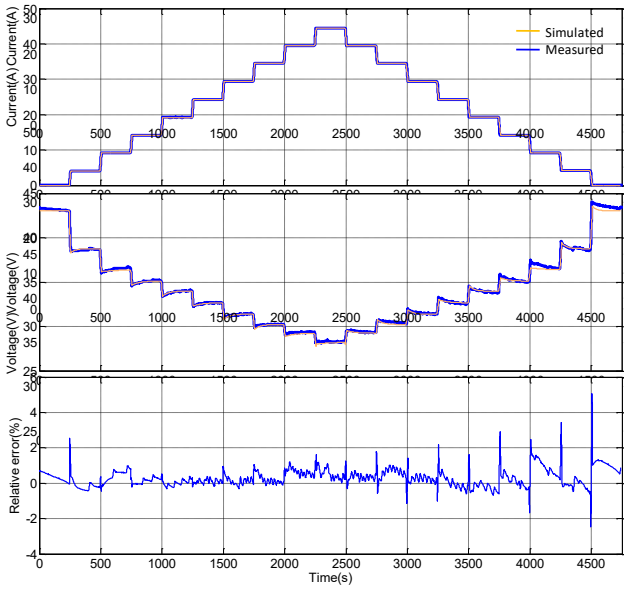

Fig. 25 Nexa fuel cell experimental and model simulation results, applying current increments of 11% load range.

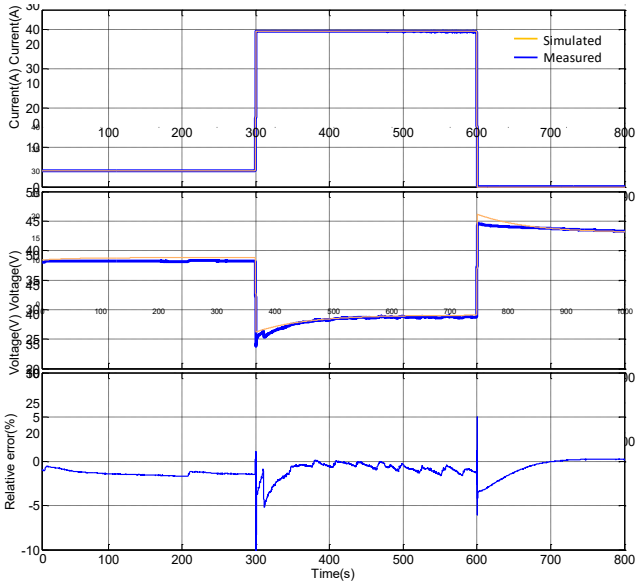

Fig. 26 Nexa fuel cell experimental and model simulation results, applying current increments of 77% and 88% load range.

V. Conclusion

A PEM fuel cell black-box model with overshooted transient response and its identification methodology have been presented in this paper. The proposed fuel cell model consists of a small number of components: the static fuel cell model comprises only two resistors, whereas the dynamic fuel cell model needs, besides the previous components, another resistor, an inductance and a capacitor.

It is remarkable that both the static model and the dynamic model can be parameterized independently. The dynamic model not only reproduces the slower physical phenomena inside the fuel cell, but also the faster ones associated with the double capacitive layer effect. The use of variable resistors in the fuel cell model allows implementing a variable time constant depending on the fuel cell current. Additionally, the facilities needed for the fuel cell measurements and identification are simple, just obtaining the fuel cell transient response when a set of load steps is applied is enough in order to identify the model dynamic parameters. The identification methodology uses a reduced number of steps, and the required equations are very easy to implement.

The dynamic model components parameterization does not need a large number of points and the relative error between the experimental and simulated data is in general lower than ±2%.

Also, the fuel cell frequency response has been described, detailing the dynamic components influence, and it has been

presented an independent analysis for low and high frequencies. With the developed frequency response analysis, the fuel cell can also be parameterized if the transient response is not available.

Finally, the analyzed experimental results show a very good accuracy when the model simulation results are compared to experimental data, even when different load current sequences, different number of steps and different current increments are applied.

The proposed fuel cell model can be considered as a reference model in the design of a fuel cell emulator, due to its simplicity and accuracy.

REFERENCES

[1] J. Balakrishnan, "Fuel Cells - Configuration and Operation", in *Proc. IEEE Electrical Power Conf., 2007*, pp. 213 – 217

[2] M. Jang, M. Ciobotaru, V. Agelidis, "A Single-Phase Grid-Connected Fuel Cell System Based on a Boost-Inverter", *IEEE Trans. Power Electron*., vol. 28, no. 1, pp. 279 – 288, Jan. 2013

[3] W. Liu, J. Chen, T. Liang, R. Lin, "Multicascoded Sources for a High-Efficiency Fuel-Cell Hybrid Power System in High-Voltage Application", *IEEE Trans. Power Electron*., vol. 26, no. 3, pp. 931 - 942, March 2011

[4] L. Luckose, H. Hess, B. Johnson, "Fuel cell propulsion system for marine applications", *Electric Ship Technologies Symposium, 2009,* pp. 574 - 580

[5] P. Garcia, L. Fernandez, C. Garcia, F. Jurado, "Energy Management System of Fuel-Cell-Battery Hybrid Tramway ", *IEEE Trans. Industrial Electron.,* vol. 57, no. 12, pp. 4013 – 4023, Dec. 2010

[6] E. Bataller-Planes, N. Lapea-Rey, J. Mosquera, F. Orti, J. A. Oliver, O. Garcia, F. Moreno, J. Portilla, Y. Torroja, M. Vasic, S. C. Huerta, M. Trocki, P. Zumel, J. A. Cobos, "Power balance of a hybrid power source in a power plant for a small propulsion aircraft", *IEEE Trans. Power Electron.*, vol. 24, no. 12, pp.2856 -2866, Dec. 2009

[7] A. Emadi, S. Williamson, A. Khaligh, "Power electronics intensive solutions for advanced electric, hybrid electric, and fuel cell vehicular power systems", *IEEE Trans. Power Electron*., vol. 21, no. 3, pp.567 - 577, May 2006

[8] M. Guarnieri, V. Di Noto, F. Moro, "A Dynamic Circuit Model of a Small Direct Methanol Fuel Cell for Portable Electronic Devices", *IEEE Trans. Industrial Electron.,* vol. 57, no. 6, pp. 1865 – 1873, Jun. 2010

[9] C. ern nde , P. Zumel, V. Valdivia, A. ern nde -Herrero, M. Sanz, A. L aro, A. Barrado, "Simple Model and Experimental Identification of a Fuel-Cell-Based Power Supply Oriented to System-Level Analysis", *IEEE Trans. Power Electron.,* vol. 26, no. 7, pp. 1868-1878, July 2011

[10] A. Kirubakaran, S. Jain, R. Nema, "DSP-Controlled Power Electronic Interface for Fuel-Cell-Based Distributed Generation", *IEEE Trans. Power Electron.*, vol. 26, no. 12, pp.3853 -3864, Dec. 2011

[11] J. Cao, A. Emadi, "A New Battery/UltraCapacitor Hybrid Energy Storage System for Electric, Hybrid, and Plug-In Hybrid Electric Vehicles", *IEEE Trans. Power Electron.*, vol. 27, no. 1, pp.122 -132, Jan. 2012

[12] G. Zhu, S. Tan, Y. Chen, C. Tse, "Mitigation of Low-Frequency Current Ripple in Fuel-Cell Inverter Systems Through Waveform Control", *IEEE Trans. Power Electron.*, vol. 28, no. 2, pp.779 -792, Feb. 2013

[13] O. Hega y, J. Van Mierlo, P. Lataire, "Analysis, Modeling, and Implementation of a Multidevice Interleaved DC/DC Converter for Fuel Cell Hybrid Electric Vehicles", *IEEE Trans. Power Electron.*, vol. 27, no. 11, pp.4445 -4458, Nov. 2012

[14] C. Raga, A. Barrado, I. Quesada, A. Lazaro, C. Anocibar, J.F. Sierra, "Analysis and comparison of four regenerative power distribution architectures based on fuel cell, supercapacitors and batteries", in *Proc. IEEE Industrial Electronics Conf.,* 2008*,* pp. 545 - 550

[15] C. Raga, A. Barrado, I. Quesada, A. Lazaro, C. Anocibar, J.F. Sierra, "Comparison of two different electrical power architecture for electric vehicles applications based on Fuel Cell and supercapacitors ", *in Proc. IEEE Power Electronics Specialists Conf.,* 2008, pp. 1326 - 1330

[16] W. Zhang, D. Xu, X. Li, R. Xie, H. Li, D. Dong, C. Sun, M. Chen, "Seamless Transfer Control Strategy for uel Cell Uninterruptible Power Supply System", *IEEE Trans. Power Electron.*, vol. 28, no. 2, pp.717 -729, Feb. 2013

[17] R. Wai, S. Jhung, J. Liaw, Y. Chang, "Intelligent Optimal Energy Management System for Hybrid Power Sources Including Fuel Cell and Battery", *IEEE Trans. Power Electron.,* vol. 28, no. 7, pp. 3231- 3244, July 2013

[18] K. Sedghisigarchi, A. Feliachi, "Dynamic and transient analysis of power distribution systems with fuel Cells-part II: control and stability enhancement", *IEEE Trans. Energy Conversion,* vol. 19, no. 2, pp. 429 – 434, Jun. 2004

[19] G. Fontes, C. Turpin, S. Astier, T. A. Meynard, "Interactions Between Fuel Cells and Power Converters: Influence of Current Harmonics on a Fuel Cell Stack", *IEEE Trans. Power Electron.,* vol. 22, no. 2, pp. 670 – 678, Mar. 2007

[20] G. Fontes, C. Turpin, S. Astier, "A Large-Signal and Dynamic Circuit Model of a H_2/O_2 PEM Fuel Cell: Description, Parameter Identification, and Exploitation", *IEEE Trans. Industrial Electron.,* vol. 57, no. 6, pp. 1874 – 1881, Jun. 2010

[21] W. Friede, S. Rael, B. Davat, "Mathematical model and characterization of the transient behavior of a PEM fuel cell", *IEEE Trans. Power Electron.*, vol. 19, no. 5, pp.1234 -1241, Sep. 2004

[22] S. M. Njoya, O. Tremblay, L. A. Dessaint, "A generic fuel cell model for the simulation of fuel cell power systems", *in Proc. IEEE Power & Energy Society General Meeting,* 2009, pp. 1-8

[23] M. Purmann, G. Heideck, Z. Styc ynski, "Extended model for the dynamic simulation of a PEM fuel cell in stationary applications", *in Proc. IEEE Power Tech*, 2005, pp. 1-6

[24] W. Hankache, S. Caux, D. Hissel, M. adel, "Simplified electrical model tuned for actual controlled PEM C", *in Proc. IEEE Vehicle Power and Propulsion Conference, 2006,* pp. 1-6

[25] F. Gao, B. Blunier, A. Miraoui, A. El-Moudni, "A multiphysic dynamic 1D model of a proton exchange membrane fuel cell stack for real time simulation". *IEEE Trans. on Industrial Electronics*, vol. 57, no. 6, pp. 1853-1864, Jun. 2010

[26] F. Gao, B. Blunier, A. Miraoui, A. El-Moudni, "PEM uel Cell Multi-physical Dynamic Effect and Stack Spatial Non-uniformity Analysis", *Journal of Power Sources*, 195 (22): pp. 7609-7626, 2010

[27] V. Valdivia, A. Barrado, A. Lázaro, M. Sanz, D. López del Moral, C. Raga; "System-Level Black-Box Modeling of DC-DC Converters with Input Current Control for Fuel Cell Power Conditioning", *Proc. IEEE Applied Power Electronics Conf. and Exposition,* 2012*,* pp. 443-450

[28] C. A. Ramos-Paja, R. Giral, L. Martinez-Salamero, J. Romano, A. Romero, G. Spagnuolo, "A PEM Fuel-Cell Model Featuring Oxygen-Excess-Ratio Estimation and Power-Electronics Interaction", *IEEE Trans. Industrial Electron.,* vol. 57, no. 6, pp. 1914 - 1924, Jun. 2010

[29] Boscaino, V. ; Capponi, G. ; Livreri, P. ; Marino, . " uel cell modelling for power supply systems design", *in Proc. IEEE Control and Modeling for Power Electronics*, 2008, pp. 1-4

[30] X. Kong, A. M. Khambadkone, S. K. Thum, "A hybrid model with combined steady-state and dynamic characteristics of PEMFC fuel cell stack", *in Proc. IEEE Industry Applications Conference*, 2005, vol. 3, pp. 1618 – 1625

[31] A. Askarzadeh, A. Re a adeh, "An Innovative Global Harmony Search Algorithm for Parameter Identification of a PEM uel Cell Model", *IEEE Trans. Industrial Electron.,* vol. 59, no. 9, pp. 3473-3480, Sept. 2012

[32] C. Raga, A. Barrado, A. Lazaro, C. Fernandez, V. Valdivia, I. Quesada, "Black-box model and identification methodology for PEM fuel cell with overshooted transient response", *in Proc. IEEE Energy Conversion Congress and Exposition,* 2012*,* pp. 3168 - 3174

[33] K. P. Adzakpa, K. Agbossou, Y. Dube, M. Dostie, M. Fournier, A. Poulin, "PEM Fuel Cells Modeling and Analysis Through Current and Voltage Transient Behaviors", *IEEE Trans. Energy Conversion,* vol. 23, no. 2, pp. 581-591, Jun. 2008

[34] C. Wang, M. H. Nehrir, S. R. Shaw, "Dynamic models and model validation for PEM fuel cells using electrical circuits", *IEEE Trans. Energy Conversion,* vol. 20, no. 2, pp. 442-451, Jun. 2005

[35] http://www.mathworks.es/

[36] A. Forrai, H. Funato, Y. Yanagita, Y. Kato, "Fuel-Cell Parameter Estimation and Diagnostics", *IEEE Trans. Energy Conversion,* vol. 20, no. 3, pp. 668 – 675, Sept. 2005

[37] A. M. Dhirde, N. V. Dale, H. Salehfar, M. D. Mann, T. H. Han, "Equivalent Electric Circuit Modeling and Performance Analysis of a PEM Fuel Cell Stack Using Impedance Spectroscopy", *IEEE Trans. Energy Conversion,* vol. 25, no. 3, pp. 778 - 786, Sept. 2010

[38] W. Choi, P. N. Enjeti, J. W. How e, "Development of an equivalent circuit model of a fuel cell to evaluate the effects of inverter ripple

current“, *in Proc. IEEE Applied Power Electronics Conference and Exposition,* 2004*,* pp. 355 - 361
[39] L. Gauchia, J. San , “A Per-Unit Hardware-in-the-Loop Simulation of a Fuel Cell/Battery Hybrid Energy System“, *IEEE Trans. Industrial Electron.,* vol. 57, no. 4, pp. 1186 - 1194, Apr. 2010
[40] S. C. Page, A. H. Anbuky, S. P. Krumdieck, J. Brouwer, "Test Method and Equivalent Circuit Modeling of a PEM Fuel Cell in a Passive State“, *IEEE Trans. Energy Conversion,* vol. 22, no. 3, pp. 764-773, Sept. 2007
[41] http://www.powersimtech.com/
[42] http://www.dspace.com/

Carmen Raga was born in Madrid, Spain, in 1976. She received her M. Sc in electrical engineering in 2005 from the Carlos III University of Madrid, Spain. She has been involved in power electronics research and development projects since 2002 within the Power Electronics Systems Group of the Carlos III University of Madrid (GSEP). From 2005 onward she has been an Assistant Professor at the Electronic Department of the Carlos III University of Madrid, Spain.
Her main research interests are switched-mode power supplies modeling and control, fuel cells and power distribution architectures for hybrid electrical vehicle applications.
She is a member of the IEEE Power Electronics Society (PELS) and the IEEE Industrial Electronics Society (IES).

Andrés Barrado was born in Badajoz, Spain, in 1968. He received the M. Sc. degree in electrical engineering from Polytechnic University of Madrid, Spain, in 1994, and the Ph.D. degree from Carlos III University of Madrid, Spain, in 2000. He is Professor at Carlos III University of Madrid, and since 2004 Head of the Power Electronics Systems Group (GSEP). His research interests are: switching-mode power supply, inverters, power factor correction, solar and fuel cell conditioning, behavioural modelling of converters and systems, fuel cell electric vehicle (FCEV) and power distribution systems for aircrafts. He has published over 150 scientific papers in international journals and conference proceedings and holds 11 patents. He has been actively involved in over 65 R&D projects for companies in Europe and the U.S.
Dr. Barrado is a member of the IEEE-PELS-IES Spanish Chapter.

Antonio Lázaro was born in Madrid, Spain, in 1968. He received the M. Sc. in electrical engineering from the Universidad Politécnica de Madrid, Spain, in 1995. He received the Ph. D. in Electrical Engineering from the Universidad Carlos III de Madrid in 2003.
He has been an Assistant Professor of the Universidad Carlos III de Madrid since 1995. He has been involved in power electronics since 1994, participating in more than 50 research and development projects for industry. He holds seven patents and software registrations and he has published nearly 125 papers in IEEE journals & conferences. His research interests are switched-mode power supplies, power factor correction circuits, inverters (ups and grid connected applications), modeling and control of switching converters and digital control techniques.

Cristina Fernández (M’05) received the M.S. and Ph.D. degrees in electrical engineering from the Universidad Politecnica de Madrid (UPM), Madrid, Spain, in 1998 and 2004, respectively. From 1997 to 2003 she was a Researcher at the UPM, joining General Electric CR&D (Niskayuna, New York, USA) for a summer internship in 2000. Since 2003, she has been with the Carlos III University of Madrid (Spain), where she is currently an Assistant Professor in the Department of Electronic Technology. Her current research interests include modular DC-DC converters, techniques for measuring the frequency response of switched-mode power supplies, automatic design of compensators and educational issues on power electronics. She is currently an Associate Editor for the IEEE Transactions on Power Electronics.

Virgilio Valdivia was born in Barcelona, Spain, in 1983. He received the M.Sc. and Ph.D. degree in electrical engineering from Carlos III University of Madrid, Leganés, Spain, in 2006 and 2013, respectively. From 2006 to 2012, he was with the Carlos III University of Madrid as a Research Engineer. Since 2012, he has been with United Technologies Research Center Ireland, Cork, as a Senior Research Engineer. He has also been a visiting researcher at the European Space Research and Technology Centre in 2009, the Rolls Royce University Technology Centre of the University of Manchester in 2011, and the Center for Power Electronics Systems at Virgina Tech in 2012.
His research interest includes modeling, identification and control of power electronics converters, energy microgrids and aerospace systems.

Isabel Quesada was born in Madrid, Spain, in 1977. She received her M. Sc in electrical engineering in 2005 from the Carlos III University of Madrid, Spain. She received the Ph. D. in Electronic Engineering from the Universidad Carlos III de Madrid in 2011.
She has been involved in power electronics research and development projects since 2002 within the Power Electronics Systems Group of the Carlos III University of Madrid (GSEP). From 2005 onward she has been an Assistant Professor at the Electronic Department of the Carlos III University of Madrid, Spain.
Her main research interests are auxiliary railway power supplies, inverters, modulation techniques for power converters and switched-mode power supplies modeling and control.
She is a member of the IEEE Power Electronics Society (PELS) and the IEEE Industrial Electronics Society (IES).

Lucia Gauchia (M’08) received the General Engineering degree and the Ph.D. degree in Electrical Engineering from the University Carlos III of Madrid, Spain in 2005 and 2009, respectively.
Since August 2013 she is the Richard and Elizabeth Henes Assistant Professor of Energy Storage Systems at the Electrical and Computer Engineering Department and Mechanical Engineering-Engineering Mechanics Department at Michigan Technological University (USA). During 2012 she was a Postdoctoral Research Associate with McMaster University (Canada), working for the Canada Excellence Research Chair in Hybrid Powertrain and the Green Auto Powertrain Program. From 2008 to 2012 she worked at the Power Electric Engineering Department at the University Carlos III of Madrid (Spain).
Her research interests include the testing, modeling and energy management of energy storages systems and fuel cells, for microgrid and electrical vehicle applications.